Cadmium transport in sediments by tubificid bioturbation: An assessment of model complexity

Sebastien Delmotte, Filip J.R. Meysman, Aurélie Ciutat, Alain Boudou, Sabine Sauvage, Magali Gérino

Cadmium transport in sediments by tubificid bioturbation: An assessment of model complexity

Sebastien Delmotte [a,*], Filip J.R. Meysman [c], Aurelie Ciutat [b], Alain Boudou [b], Sabine Sauvage [a], Magali Gerino [a]

[a] *Laboratoire d'Ecologie des Hydrosystémes (LEH), UMR CNRS UPS 5177, Université Toulouse 3, 29 rue Jeanne Marvig, 31055 Toulouse Cedex 04, France*
[b] *Laboratoire d'Ecophysiologie et Ecotoxicologie des Systèmes Aquatiques (LEESA), UMR CNRS 5805, Université Bordeaux 1, Place du Docteur Peyneau, 33120 Arcachon, France*
[c] *The Netherlands Institute of Ecology (NIOO-KNAW), Centre for Estuarine and Marine Ecology, Korringaweg 7, 4401 NT Yerseke, The Netherlands*

Abstract

Biogeochemistry of metals in aquatic sediments is strongly influenced by bioturbation. To determine the effects of biological transport on cadmium distribution in freshwater sediments, a bioturbation model is explored that describes the conveyor-belt feeding of tubificid oligochaetes. A stepwise modelling strategy was adopted to constrain the many parameters of the model: (i) the tubificid transport model was first calibrated on four sets of microspheres (inert solid tracer) profiles to constrain tubificid transport; (ii) the resulting transport coefficients were subsequently applied to simulate the distribution of both particulate and dissolved cadmium. Firstly, these simulations provide quantitative insight into the mechanism of tubificid bioturbation. Values of transport coefficients compare very well with the literature, and based on this, a generic model of tubificid bioturbation is proposed. Secondly, the application of the model to cadmium dataset sheds a light on the behaviour of cadmium under tubificid bioturbation. Cadmium enters the sediment in two ways. In one pathway, cadmium enters the sediment in the dissolved phase, is rapidly absorbed onto solid particles, which are then rapidly transported to depth by the tubificids. In the other pathway, cadmium is adsorbed to particles in suspension in the overlying water, which then settle on the sediment surface, and are transported downwards by bioturbation. In a final step, we assessed the optimal model complexity for the present dataset. To this end, the two-phase conveyor-belt model was compared to two simplified versions. A solid phase-only conveyor-belt model also provides good results: the dissolved phase should not be explicitly incorporated because cadmium adsorption is fast and bioirrigation is weak. Yet, a solid phase-only biodiffusive model does not perform adequately, as it does not mechanistically capture the conveyor-belt transport at short time-scales.
© 2006 Elsevier Inc. All rights reserved.

1. Introduction

The reworking activities of benthic organisms exert a crucial control on the transport and fate of contaminants in aquatic sediments (Banta and Andersen, 2003). Solute transport (enhanced diffusion, bioirrigation, and advective irrigation) and particle transport (biodiffusion, bioadvection, biodeposition, and bioresuspension) enhance the transfer of contaminants both from sediments to overlying water and from the overlying water to the sediment. These opposite effects depend on the physico-chemical conditions and the faunal species involved. On the one hand, bioturbation increases accumulation of pollutants in sediments and stimulates their microbial degradation, and on the other hand, bioturbation and especially bioirrigation, enhance the mobility of pollutants and hence their release out of the sediment.

Human activity has mobilized trace metals from mineral deposits, and this has led to an enrichment of these

* Corresponding author. Fax: +33 562269999.
E-mail address: sebastien.delmotte@cict.fr (S. Delmotte).

compounds in aquatic environments, with sometimes toxic consequences for the local biota. Cadmium is an important contaminant in freshwater ecosystems where sediments act as a final sink. Like other metallic contaminants, cadmium displays a complex chemistry, where sorption and precipitation/dissolution are governed by a complex set of environmental controls like temperature, oxygen, pH, grain size, and sediment composition (Fu and Allen, 1992; Warren and Haack, 2001). Bioturbation interferes significantly with this chemistry: it modifies the partitioning between solid and dissolved phases (Vale and Sundby, 1998), as well it changes the transfer between sediments and overlying water (Banta and Andersen, 2003). However, the complex interaction between biological transport and cadmium chemistry often impedes the straightforward interpretation and generalization of experimental observations. Soster et al. (1992) and Petersen et al. (1998) demonstrated that bioturbation increases the cadmium and zinc fluxes from overlying water to uncontaminated estuarine or freshwater sediments. Yet, Rasmussen et al. (1998, 2000) observed that *Arenicola marina* increased the net transport of cadmium from overlying water to the sediment when the water is contaminated, but reduced the release of cadmium from contaminated sediments to overlying water that is not contaminated.

Here, we investigate whether and how reactive transport modelling can improve our understanding of the interaction between bioturbation and trace metal geochemistry. An important issue in this concerns the complexity of the proposed model formulation: how detailed should one describe both the biological transport and the trace metal chemistry in order to arrive at a suitable characterization of trace metal behaviour under the influence of bioturbation? To address this topic, we present a model analysis of the experimental work previously published by Ciutat et al. (2005a,b) on the effects of tubificid bioturbation on cadmium (Cd) dynamics. Tubificid oligochaetes are often dominant bioturbators in freshwater sediments and show a remarkable resistance to hypoxic conditions. Solid transport by tubificids results from so-called conveyor-belt feeding, where sediment material is ingested at depth and deposited as faecal pellets at the sediment–water interface (SWI). In the past a number of conveyor-belt models have been proposed to describe tubificid bioturbation (Fisher et al., 1980; Boudreau, 1986b; Rice, 1986; Robbins, 1986).

Our aim is to perform a systematic analysis of these conveyor-belt models, and show how such a model can be used to provide additional insights about empirical data that cannot be easily obtained from experimental observations alone. Past modelling studies have been typically applied to a single tracer with a well-defined reactive behaviour, usually a single radionuclide. Here, we employ the conveyor-belt model to analyse a more extensive dataset that contains data on both inert particles (microspheres) as well dissolved and particulate cadmium. We then critically assess the complexity of the conveyor-belt model. In other words, we ask whether a more complex description (with

an increased number of parameters) would enable a better fit, or whether is it possible to reduce the complexity of the present model and still keep a good agreement with data. Three relevant questions are investigated: (i) Must the dissolved cadmium phase be modelled explicitly? (ii) How important is the small-scale mixing in tubificid bioturbation? (iii) Can a simple biodiffusive model be an alternative sufficient to describe the cadmium diagenesis? The overall result is a systematic and stepwise application of a model to the available data, which exposes those aspects of tubificid bioturbation that are principally influencing the fluxes and distribution of cadmium.

2. Model formulation

2.1. Reactive transport equations

The biogeochemical model presented here is an adaptation of the conveyor-belt bioturbation models presented in Fisher et al. (1980), Robbins (1986), and Rice (1986). The general theory of reactive transport in surface sediments can be found in Berner (1980) and Boudreau (1997). Our model incorporates two solid species (inert luminophores called "microspheres" and adsorbed cadmium) and one solute (cadmium dissolved in the pore water). The mass conservation equation for the two solid species is of the form

$$\frac{\partial C_s}{\partial t} = \frac{\partial}{\partial x}\left[D_b(x)\frac{\partial C_s}{\partial x}\right] - \frac{\partial}{\partial x}[\omega_b(x)C_s] - k_b(x)C_s + R_s, \quad (1)$$

where x represents the depth into the sediment (cm), t is time (yr), C_s is the solid concentration (μmol g^{-1} of dry sediment), and R_s is the production rate due to reactions (μmol g^{-1} of dry sediment yr^{-1}).

Similarly, the mass balance for the solute becomes

$$\frac{\partial C_f}{\partial t} = \frac{\partial}{\partial x}\left[(D_b(x) + D_m)\frac{\partial C_f}{\partial x}\right] - \frac{\partial}{\partial x}[\omega_b(x)C_f]$$
$$- k_b(x)C_f + R_f, \quad (2)$$

where C_f is the solute concentration (μmol L^{-1} pore water) and R_f is the production rate due to reactions (μmol L^{-1} pore water yr^{-1}). The parameter D_m denotes the effective diffusivity in the pore water (cm^2 yr^{-1}), which is calculated from the molecular diffusion coefficient D_0 by the application of the tortuosity correction (Boudreau, 1997):

$$D_m = \frac{D_0}{1 - \ln(\varphi^2)}, \quad (3)$$

where φ denotes the porosity, which is considered constant with depth. Sediment was homogenized prior to the incubations, and we assume that no significant porosity gradients will develop during the incubations.

Both the mass balances (1) and (2) are of the classical advection–diffusion–reaction form. In these, the subscripts "s" and "f", respectively, denotes the solid phase and the fluid phase. The parameters with subscript "b" represent

the biological transport induced by the deposit-feeding of tubificid oligochaetes. This transport is modelled as a superposition of two effects: (i) a conveyor-belt mechanism, where the sink coefficient k_b models the ingestion rate at depth and the bioadvective velocity ω_b (cm yr^{-1}) models the resulting downward transport of overlying sediment, and (ii) a small-scale mixing mechanism represented by the biodiffusion coefficient D_b. Biological activity changes significantly with depth, and as a result, all three biological transport parameters k_b, ω_b, and D_b are made depth dependent. Biodiffusion decreases with depth according to the relation:

$$D_b(x) = D_b^0 \exp\left[-\frac{1}{2}\left(\frac{x}{x_{mix}}\right)^2\right], \tag{4}$$

where D_b^0 is the mixing intensity at the sediment–water interface (cm^2 yr^{-1}), and the attenuation coefficient x_{mix} represents a characteristic mixing depth (cm). The ingestion rate is modelled by the Gaussian function:

$$k_b(x) = k_{ing}^{max} \exp\left[-\frac{(x - x_{ing})^2}{2\sigma_{ing}^2}\right], \tag{5}$$

where k_{ing}^{max} is the maximal ingestion rate (yr^{-1}), x_{ing} is the mean depth where tubificids are deposit-feeding (cm), and σ_{ing} is the square root variance of this ingestion depth (cm). The ingestion relation (5) can be justified if we assume that the population of tubificids has a normal size distribution, and the size of the organisms linearly scales with the depth at which they feed. Downward bioadvection is a consequence of the removal of sediment at depth by conveyor-belt deposit-feeding. The bioadvective velocity is obtained from a mass balance for the bulk sediment (Boudreau, 1997)

$$\omega_b(x) = \int_x^L k_b(x)\mathrm{d}x \tag{6}$$

where L represents the depth of the model domain (cm). Eqs. (4)–(6) provide a model for the conveyor-belt transport of tubificids that incorporates five parameters in total $(D_b^0, x_{mix}, x_{ing}, k_{ing}^{max}, \sigma_{ing})$. These parameters need to be constrained by appropriate comparison of model simulations with tracer data.

Our treatment of the biological transport is identical to that of Robbins (1986), except that we do not include particle size selectivity. As we will further see, the tracer data of Ciutat et al. (2005a,b) do not allow the investigation of this aspect, as one needs particulate tracers of at least two size classes. Robbins' assumption of steady-state compaction is not relevant for the present experimental conditions here, as sediment was homogenized prior to the incubations (eradicating any porosity gradients). Hence the porosity must be approximated as constant with depth, or it should be fully modelled in a transient manner. The latter approach should then account for the effect of tubificid bioturbation on compaction. Given the complex im-

pact of bioturbation on compaction (Meysman et al., 2005), and the poor knowledge about how tubificids affect on porosity (Ciutat et al., 2006), the transient modelling approach was not realistic. Also note that the treatments of Robbins (1986) incorrectly represent the effect of bioturbation on porosity. Biodiffusion was included as an interphase mixing process, which has recently been shown incorrect under the assumption of steady-state compaction (Meysman et al., 2005).

Solute transport resulting from burrow flushing, conventionally represented by a nonlocal exchange function, is not included in Eq. (2). Although bioirrigation is recognized as a major transport mechanism for other conveyor-belt feeders such as lugworms (Timmermann et al., 2003; Meysman et al., 2006a,b), or for gallery dwellers such as chironomids (Stief and De Beer, 2002), studies about tubificid bioirrigation present somewhat contradictory conclusions. Several authors have argued that tubificid bioirrigation is negligible (McCall and Fisher, 1980; Kresoski and Robbins, 1981). According to Wood (1975), the tubificid *Limnodrillus hoffmeisteri* generates a burrow flushing rate of 9.5–15 µL water per worm per hour (20 °C). At typical densities of 10^4–10^5 ind m^{-2}, this would result in exchange of 25 L m^{-2} d^{-1}, which is important, but not massively high when compared to *Nereis divercolor* populations, which may induce 1500 L m^{-2} d^{-1} (Kristensen and Kostka, 2005). Wang and Matisoff (1997) used ^{22}Na to monitor the bioirrigation induced by the tubificid *Branchiura sowerbyi*, and reported a diffusion enhancement factor in the range from 2 to 5. Here, bioirrigation is not included for two main reasons: (i) incubations were not carried with a conservative solute, and hence, no independent data is available to constrain the parameters in a bioirrigation process model, and (ii) *a posteriori* we will show that solute transport will have a negligible influence on the simulations, which represents one of the major conclusions in this study.

In the simulations of the inert microspheres, the reaction term in the solid mass balance (1) is set to zero. In the simulations of cadmium dispersal, standard adsorption kinetics are implemented to describe the sorptive behaviour. At equilibrium, the concentration of particulate cadmium is linked to the concentration of dissolved cadmium by the linear adsorption isotherm

$$C_s^{eq} = K_p C_f^{eq}, \tag{7}$$

where K_p represents the partitioning coefficient (L g^{-1} of dry sediment). Accordingly, the reaction term for the adsorbed cadmium thus becomes

$$R_s = k_{ad}(K_p C_f - C_s), \tag{8}$$

where k_{ad} represents a kinetic rate constant of sorption (yr^{-1}). Accounting for the volume ratio of both pore water and solid sediment, the corresponding reaction term for dissolved cadmium is directly calculated as

$$R_f = -R_s \rho_s (1 - \varphi)/\varphi, \tag{9}$$

where ρ_s is the density of the solid sediment (g L^{-1}) and φ is the porosity. The partitioning constant K_p was kept constant with depth, as the exchange between solid and dissolved cadmium phases is primarily controlled by redox conditions (Jacobs and Emerson, 1982), and the tubificids did not change the oxygenation of the sediment in the simulated experiments. With and without worms, oxygen was observed to attain a similar penetration depth of 3–5 mm (Ciutat et al., 2005b). Moreover, tubificids are not known to line their burrows with mucus, and hence, there are no indications of preferential cadmium adsorption near the burrow walls.

2.2. Boundary conditions

Microspheres are deposited as a thin layer on the sediment surface, and subsequently, the down-mixing of this "pulse" is followed through time. We idealize the initial conditions as a Dirac delta function at the SWI, and during the simulations both the upper and lower model domain are modelled as impenetrable (no-flux condition). In the cadmium experiments the dissolved cadmium concentration in the water column was re-adjusted daily to a fixed level to maintain a constant contamination pressure. In the simulations we adopted the fixed concentration condition:

$$C_f = C_f^0 \tag{10}$$

where C_f^0 denotes the daily-averaged concentration in the overlying water, which remained constant in time. For the particulate cadmium, we impose the flux $F_s^0(t)$ (μmol cm^{-2} yr^{-1}) that crosses the SWI. This leads to the flux condition

$$F_s^0(t) = -\rho_s(1-\varphi)D_b(0)\frac{\partial C_s}{\partial x}\bigg|_{x=0} + \rho_s(1-\varphi)\omega_b(0)C_s(0,t). \tag{11}$$

The calculation of the function $F_s^0(t)$ is discussed in detail. At the lower boundary, the experimental core set-up is sealed, and hence, we assume a no-gradient condition for both the particulate and dissolved cadmium

$$\frac{\partial C_s}{\partial x}\bigg|_{x=L} = \frac{\partial C_f}{\partial x}\bigg|_{x=L} = 0. \tag{12}$$

2.3. Flux calculations

In order to construct a mass balance for all cadmium in the set-up, we need a proper quantification of the various fluxes across the SWI (all in μmol cm^{-2} yr^{-1}). The deposit-feeding activity of the tubificids will result in a "biological" flux F_f^b of dissolved cadmium from the pore water to the overlying water. We assume that deposit-feeding removes whole volume packages at depth, and consequently, dissolved cadmium is removed from the pore water at the rate

$$F_f^b(t) = \varphi \int_0^L k_b(x)C_f(x,t)dx. \tag{13}$$

In contrast to Robbins (1986), we assume that the transported pore water immediately mixes with overlying water. Indeed, tubificids are known to let the posterior part of their body out of their burrows, and to make circular movements in the overlying water. Accordingly, the dissolved cadmium that is brought up will disperse in the overlying water, and will not re-enter through the SWI as assumed by Robbins (1986). The net flux of dissolved cadmium across SWI is denoted F_f^{net}, and thus can be calculated as the difference between two separate contributions

$$F_f^{net}(t) = F_f^{ext}(t) - F_f^b(t). \tag{14}$$

The contribution $F_f^{ext}(t)$ represents the transfer of dissolved cadmium from the "external" overlying water to the pore water across the SWI. For reasons of mass conservation, it should match the advective–diffusive flux $F_f^0(t)$ at the sediment side of the SWI

$$F_f^{ext}(t) = F_f^0(t) = -\varphi(D_b^0 + D_m)\frac{\partial C_f}{\partial x}\bigg|_{x=0} + \varphi\omega_b(0)C_f^0. \tag{15}$$

When a simulation is finished, and a profile $C_f(x)$ is available, Eq. (13) allows the calculation of $F_f^b(t)$ and Eq. (15) that of $F_f^{ext}(t)$. The net transfer of dissolved cadmium across the SWI is then calculated via (14) as the difference between these two quantities.

The calculation procedure for the fluxes of particulate cadmium is different from that of the dissolved fraction. The advective–diffusive flux $F_s^0(t)$ cannot be calculated *a posteriori* (i.e., after a simulation as was done in (15) for dissolved cadmium), as its value is needed *a priori* to implement the boundary condition (11). However, $F_s^0(t)$ can be written as the summation of two other fluxes

$$F_s^0(t) = F_s^{ext}(t) + F_s^b(t). \tag{16}$$

The external flux $F_s^{ext}(t)$ now represents the transfer from the water column to the particulate phase of the sediment, and originates from the adsorption of dissolved cadmium in the overlying water, either directly onto the surface sediment or onto suspended particles that subsequently settle on the surface. The function $F_s^{ext}(t)$ is an input to the model (see below). The biological flux F_s^b results from the deposit-feeding activity of the tubificids: particulate cadmium is ingested at depth, and deposited back at the SWI. Similar to (13), this input can be calculated as

$$F_s^b(t) = \rho_s(1-\varphi) \int_0^L k_b(x)C_s(x,t)dx. \tag{17}$$

The principal difference between the dissolved and particulate biological fluxes (13) and (17) is that the particulate cadmium immediately returns as an input to the sediment, while the dissolved cadmium is mixed within the overlying water. As a consequence, the net flux across the SWI simply becomes

$$F_s^{net}(t) = F_s^{ext}(t). \tag{18}$$

In contrast to the dissolved case (14), the net flux of particulate cadmium thus solely arises from the "external" input. The net total flux across the SWI thus becomes

$$\begin{aligned} F_{tot}^{net}(t) &\equiv F_s^{net}(t) + F_f^{net}(t) \\ &= F_s^{ext}(t) + \left[F_f^{ext}(t) - F_f^{b}(t) \right]. \end{aligned} \tag{19}$$

The value of F_{tot}^{net} can be constrained by monitoring the net removal cadmium from the overlying water.

2.4. Numerical solution

The simulations presented here are all transient simulations, and the simulation approach consists of three consecutive steps. In a first step, we performed a sensitivity analysis using simplified models to understand how the various modes of tubificid transport (ingestion, bioadvection, biodiffusion) affect concentration patterns. In a second step, we performed inert tracer simulations and compared these with the microsphere data to constrain the parameters that determine tubificid transport. In a third and final step, we applied these calibrated biological transport parameters in a more complex model that simulates the coupled reactive transport of both particulate and solid cadmium. In all simulations, Eqs. (1) and (2) were solved numerically using a Crank–Nicholson finite differencing scheme. The time step was fixed at 1 min and spatial resolution was to 0.01 cm, and the conservation of matter was checked. The accuracy and stability of the numerical solution was verified using analytical solutions for simplified test cases. The diffusive down-mixing of an input pulse of microspheres was tested with the analytical solution for a constant diffusion coefficient with depth (Boudreau, 1997):

$$C = \frac{1}{\sqrt{\pi D_b t}} \exp\left(-\frac{x^2}{4 D_b t}\right). \tag{20}$$

Similarly, for a solute with a constant concentration C_0 at the sediment–water interface, we applied the analytical solution for diffusion in a semi-infinite domain (Crank, 1976):

$$C = C_0 \, \text{erfc}\left(\frac{x}{2\sqrt{Dt}}\right) \tag{21}$$

Note that the numerical model adopts a finite depth L, while the analytical solutions (15) and (16) are only valid for a semi-infinite domain. So after a sufficient time, the numerical solution will "feel" the influence of the impermeable bottom, and numerical solutions will start to deviate from the analytical benchmark solutions.

3. Simulations, parameters and experimental data

3.1. Model analysis: tubificid transport modes

To assess how different tubificid transport mechanisms (ingestion, bioadvection, and biodiffusion) affect tracer profiles, we investigated three consecutive simplifications of the model detailed in Section 2. Parameters values used in these simulations are reported in Table 1. Model A incorporates all three transport mechanisms (ingestion, bioadvection, and biodiffusion) but neglects any reaction ($R_s = R_f = 0$). Model B neglects the ingestion mode of conveyor-belt transport ($k_{ing}^{max} = 0$), and thus reduces to the simple advection-diffusion model. Model C neglects conveyor-belt transport altogether (ingestion + bioadvection), and therefore, only retains biodiffusive mixing. Note that in model B, the ingestion rate is set to zero in the mass balances (1) and (2), but not in Eq. (6), in order to still obtain a non-zero bioadvection velocity. These three different models A, B and C were then used in three different scenarios. For a particulate tracer, we simulated both the transient down-mixing of a pulse input, as well as the transient development of tracer profiles after the implementation of a constant input flux. For the solute tracer, the transient development of tracer profiles was modelled using a fixed concentration in the overlying water. The parameter set that was used in models A and B reflects a typical bioturbation regime for tubificids (Fisher et al., 1980; Robbins, 1986) ($D_b^0 = 2 \text{ cm}^2 \text{ yr}^{-1}$, $x_{mix} = 2 \text{ cm}$, $k_{ing}^{max} = 5 \text{ yr}^{-1}$, $x_{ing} = 5 \text{ cm}$, and $\sigma_{ing} = 2 \text{ cm}$). In model C, the rate of mixing was increased to $D_b^0 = 30 \text{ cm}^2 \text{ yr}^{-1}$, so that over the simulated period, the particulate tracer reaches about the same depth as in the simulations of conveyor-belt transport. For the dissolved tracer, the molecular diffusion D_0 of dissolved cadmium was taken at 20 °C, i.e., 200 cm^2 yr^{-1} (Boudreau, 1997). The porosity was set to 0.74 as in the experiments of Ciutat et al. (2005a,b), and the solid density was fixed at 2.5 g cm^{-3}.

3.2. Experimental dataset

The tracer dataset that was used for model calibration and application is detailed in Ciutat et al. (2005a,b). The experimental approach was based on indoor microcosms, which featured a two-compartment biotope, containing sediment and overlying water enclosed in a glass container (inner diameter = 5.3 cm, sediment volume = 265 cm^3, overlying water volume = 110 cm^3). Glass containers were placed into thermoregulated tanks containing 24 L of water. Sediment was taken from the Garonne River (Gironde, Southwest France). The sediment was sieved through a 1-mm mesh to remove macrofauna and frozen at −20 °C to kill remaining organisms. It was then defrosted and homogenized. The background cadmium concentration was 6.7 ± 0.18 µmol kg^{-1}, and organic carbon content was 6.9%. The density of added tubificid worms (Annelida, Oligochaeta) was fixed at about 60,000 individuals m^{-2}. Three experimental treatments were studied: tubificids without cadmium {−Cd + Tub}, cadmium without tubificids {+Cd − Tub} and tubificids with cadmium {+Cd + Tub}. In each of these treatments, the transport of solid particles was quantified using fluorescent particles called microspheres (Fluoresbrite YG Microspheres,

Table 1
Parameter values used in various model simulations: sensitivity analysis, calibration of the model on microspheres profiles, and applications of the model on cadmium distributions

	ρ_s (g cm^{-3})	φ	D_0 (cm^2 yr^{-1})	D_b^0 (cm^2 yr^{-1})	x_{mix} (cm)	k_{ing}^{max} (yr^{-1})	x_{ing} (cm)	σ_{ing} (cm)	$\omega_b(0)$ (cm yr^{-1})	K_p (L g^{-1})	k_{ad} (yr^{-1})	C_f^0 (μmol L^{-1})	F_s^{ext} (μmol cm^{-2} yr^{-1})
Sensitivity analysis. Model A (Fig. 2)				2		5	5	2	25	0	0		
Sensitivity analysis. Model B (Fig. 2)			0 or 200	2		0	—	—	25	0	0	0 or 1	Tracer pulse or constant input flux
Sensitivity analysis. Model C (Fig. 2)				30		0	—	—	—	0	0		
Calibration on microspheres (Fig. 3)			0	3		13.3	5	2	66	0	0	0	Tracer pulse
Application on cadmium {+Cd − Tub} (not shown)			200	0		0	—	—	—	6.44	80	0.163	0.5
	2.5	0.74			2								
Application on cadmium {+Cd + Tub} (Fig. 4)			200	3		13.3	5	2	66	6.44	80	0.124	0.59 (7d), 1.71 (21d), 1.3 (56d)
Application on cadmium {+Cd + Tub} (Fig. 5)			200	3		13.3 (0–28d), 3 (28–56d)	5	2	66 (0–28d), 15 (28–56d)	6.44	80	0.124	1.3
Sensitivity analysis (not shown)			0	3		13.3	5	2	66	0	0	0	1.1 (7d), 2.2 (21d)
Sensitivity analysis (Fig. 6)			200	0.03–0.3–3		13.3	5	2	66	6.44	80	0.124	1.71
Sensitivity analysis (Fig. 7)			0	50		0	0	0	0	0	0	0	1.1 (7d), 2.2 (21d), 1.7 (56d)

Symbols are defined in the text. The notation "d" denotes "days".

Polysciences Europe GmbH, Eppelheim, Germany). Immediately after the mud cakes with microspheres were deposited at the sediment surface, the overlying water was spiked with cadmium, which determined time zero for contamination. The dissolved cadmium concentration in the overlying water of the two contaminated tanks ({+Cd + Tub} and {+Cd − Tub}) was initially fixed at 0.179 μmol L^{-1}. To maintain the contamination pressure throughout the experiment the overlying water in each tank was renewed daily. Over the course of 24 h, the dissolved cadmium concentration in the overlying water decreased, resulting in an average concentration of 0.124 μmol L^{-1} in the {+Cd + Tub} treatment and 0.163 μmol L^{-1} in the {+Cd − Tub} treatment over the course of the whole experiment. The experiment lasted 56 days, with five sampling times for fluorescent tracers (7, 14, 21, 28, and 56 days) and three sampling times for cadmium (7, 21, and 56 days). In addition, Ciutat et al. (2005b) measured vertical distribution of oxygen, dissolved and particulate manganese, sulphide, and sulphate. In all the simulations in this paper, the depth of the model domain was set to $L = 12$ cm, and a constant porosity equal to 0.74 was applied, as measured in the experimental set-up. Further details on analytical methods and experiments can be found in Ciutat et al. (2005a,b).

3.3. Model calibration: microspheres transport

The particle transport coefficients characterizing tubificid bioturbation were first determined from microsphere profiles, and subsequently applied in the cadmium simulations. Data profiles from the {+Cd − Tub} treatment were not relevant because no particulate transport occurred in the absence of tubificids. Accordingly, microsphere profiles in the {+Cd + Tub} and {−Cd + Tub} were simulated to calibrate biological transport parameters and to compare tubificid-induced bioturbation with and without cadmium. Calibration on microsphere profiles in the {+Cd + Tub} treatment provided transport parameters that were subsequently used to model the cadmium profiles measured in the same {+Cd + Tub} treatment.

As noted above, the tubificid bioturbational model contains five parameters in total, which allows considerable degrees of freedom when fitting data profiles (potentially leading to poorly constrained parameter values). To reduce this freedom, we fixed two parameter values based on past literature of tubificid ecology. Following Robbins (1986), the value for the spreading of the ingestion depth was set to $\sigma_{ing} = 2$ cm and the value for the mixing depth was set to $x_{mix} = 2$ cm. As a result, three parameters were left over for calibration: the mixing intensity D_b^0 at the SWI, the mean ingestion depth x_{ing}, and the maximal ingestion rate k_{ing}^{max}. These parameters were constrained for four different datasets (two treatments {+Cd + Tub} and {−Cd + Tub} with each two replicates), thus resulting in four parameter sets. Optimal values were obtained by scanning a range of values for each parameter, and determining the minimal

sum of squared errors (SQE) between simulated and measured profiles

$$SQE = \sum_{t=1}^{5} \sum_{i=1}^{n_t} \left(C_{i,t}^{data} - C_{i,t}^{model} \right)^2$$

where $C_{i,t}^{data}$ refers to the microsphere concentration at depth i at sampling time t (each depth and sampling time is given the same weight in the cost function). To enable a proper calculation of SQE, the modelled concentrations $C_{i,t}^{model}$ were averaged over the corresponding sediment slice.

3.4. Model application: cadmium biogeochemistry

In addition to the five biological transport coefficients constrained by the calibration on microspheres data, and the molecular diffusion coefficient D_0 for dissolved cadmium (fixed at 200 cm^2 yr^{-1} see above), the simulation of cadmium profiles required the fixation of five additional parameters: the concentration of cadmium in overlying water C_f^0, the initial background profiles of particulate and dissolved cadmium in the sediment $C_s(x,0)$ and $C_f(x,0)$, the partitioning coefficient K_p, the kinetic rate constant k_{ad} and the external solid flux F_s^{ext}. The Ciutat et al. (2005a,b) dataset provided values for four of these parameters:

(i) The average concentration in the overlying water was used for C_f^0, i.e., 0.124 μmol L^{-1} in the {+Cd + Tub} and 0.163 μmol L^{-1} in the {+Cd − Tub} case.

(ii) For the initial background cadmium concentrations $C_s(x,0)$ and $C_f(x,0)$ we used the profiles measured in {−Cd + Tub} treatment and averaged them over all sampling times.

(iii) The partitioning coefficient K_p was deduced from plotting the concentrations of dissolved and particulate cadmium measured in the {+Cd − Tub} and {+Cd + Tub} treatments. A consistent linear relationship was found (Fig. 1), and a value of 6.44 L g^{-1} of dry sediment for K_p was obtained by least squares regression ($R^2 = 0.9$, $p < 0.01$). The partitioning coefficient
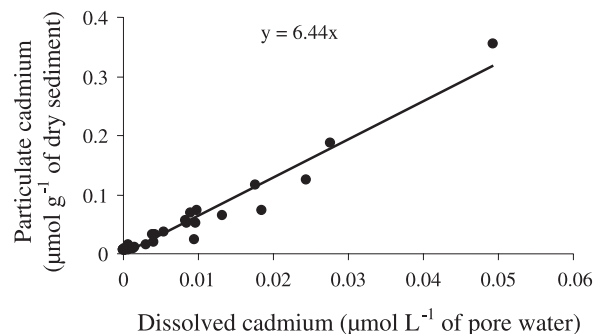

Fig. 1. Linear adsorption isotherm of cadmium. Data from {+Cd + Tub} and {+Cd − Tub} conditions were used. Linear regression provides a value of 6.44 L g^{-1} dry sediment for the partitioning coefficient K_p between liquid and solid phase ($y = 6.44x$, $R^2 = 0.9$, p value < 0.01).

was not different when analysing the data from the {+Cd − Tub} and {+Cd + Tub} treatments separately. This confirms that the presence of worms does not modify the cadmium partitioning.

(iv) The kinetic sorption constant k_{ad} was obtained from simulating the transient uploading of the sediment with cadmium in the control without tubificids {+Cd − Tub}. To this end, all biological transport parameters were set to zero in the model, and hence, a simple transient diffusion model was fitted to the cadmium profiles. A value of $k_{ad} = 80 \, yr^{-1}$ was obtained by minimisation of the sum of square errors between simulated and measured profiles of particulate and dissolved cadmium concentrations (results not shown).

The external flux F_s^{ext} could not be determined *a priori*, and hence, was calibrated on the cadmium profiles from the {+Cd − Tub} and {+Cd + Tub} treatments by a mass balance assessment. Ciutat et al. (2005b) calculated the total flux F_{tot}^{net} to the sediment (as defined in (19)) in two separate ways (i) from the increase of the cadmium inventory in the sediment and (ii) from the decrease of dissolved cadmium in the overlying water. These two methods provided similar values for F_{tot}^{net}, as required by mass conservation. In the {+Cd − Tub} treatment, Ciutat et al. (2005b) noted that F_{tot}^{net} did not vary much over time, attaining a mean value of 0.9 μmol cm^{-2} yr^{-1}. Because there is no biological transport in the {+Cd − Tub} case, the sought-after external flux of particulate cadmium can be determined as $F_s^{ext} = F_{tot}^{net} - F_f^{ext}$ from Eq. (19). The flux F_f^{ext} retained an approximately constant value of 0.4 μmol cm^{-2} yr^{-1} throughout the simulation, thus leading a constant external flux F_s^{ext} of 0.5 μmol cm^{-2} yr^{-1} In contrast, in the {+Cd + Tub} treatment, the total flux F_{tot}^{net} varied significantly trough time, and respectively amounted to 0.94, 2.04, and 1.8 μmol cm^{-2} yr^{-1} at 7, 21, and 56 days (Table 3). Because the value of F_{tot}^{net} is clearly time-dependent (Table 3), we implemented a time-dependent value interpolated the values reported by Ciutat et al. (2005b). The corresponding value for F_s^{ext} was calculated at each time step using Eq. (19).

4. Results

4.1. Model analysis: tubificid transport modes

The simulation output of the simplified models A, B, and C is presented in Fig. 2 (further referred to as the A, B, and C profiles, respectively).

4.1.1. Pulse input of inert solid (scenario 1; Fig. 2a)

As expected, model C (diffusive mixing only) simply predicts a downward smearing of the initial pulse at the SWI. The C profiles adopt the typical Gaussian shape as required by the analytical solution (20) of the diffusion equation for a pulse input. When advection is included (model B), the tracer profile initially shows the typical advection-diffusion response: the pulse migrates downward, the peak base broadens, and the peak height decreases (compare B profile at 10 and 50 days; note that profiles A and B coincide at 10 days). Strangely enough, the peak becomes sharper again after 100 days (narrower base, increased peak height). This "anomalous" peak sharpening occurs when the pulse passes the ingestion depth at 5 cm, and is a direct consequence of the decreasing bioadvective velocity within the ingestion zone. As ingestion itself is not included in model B, this then leads to the strange accumulation of tracer just below the feeding depth. Obviously, this is clearly an artefact of model B: the consequence (bioadvection) is modelled without the cause (ingestion). It is corrected in model A by the proper inclusion of tracer removal by deposit-feeding. Instead of accumulation at the feeding depth, model A shows a redistribution of tracer in the sediment above the ingestion zone. The ingestion at depth now generates a biological flux of tracer, which is deposited at the surface, and which is then buried again. This continuous process of upbringing and burial will eventually lead to a homogeneous tracer concentration in the zone above the ingestion depth.

4.1.2. Constant influx of inert solid (scenario 2; Fig. 2b)

The factors determining the tracer profiles under constant flux conditions are essentially the same as in the pulse input scenario. Model C (diffusive mixing only) leads to an exponential decreasing tracer profile, as predicted by analytical solution (21). Initially (10 days), models A and B provide exactly the same response, but once the signal reaches the ingestion zone, the A and B tracer profiles start to differ. Again, the absence of ingestion causes the anomalous accumulation of tracer at depth in model B. Consequently, the highest tracer concentrations are found at depth in the B profile. The inclusion of ingestion (model A) has the opposite effect: the combination of the biological flux together with an external input causes that tracer concentrations are highest near the SWI.

4.1.3. Constant concentration of inert solute in the overlying water (scenario 3; Fig. 2c)

Reflecting the inherent difference in transport rates, the "uploading" of the sediment with a dissolved tracer proceeds markedly faster than for a solid tracer. At 10 days, the C profile exhibits an exponential decreasing shape as predicted by the analytical solution (21). However, after 50 days, the diffusive signal has already reached the impermeable bottom of the model domain, and starts to accumulate at depth. The inclusion of bioadvection (model B) results in an enhanced accumulation of the solute at depth. This effect is again offset by the biological tracer ingestion incorporated into model A. Overall, the solute profile predicted by full biological transport model (model A) does not differ much from that generated by the purely physical transport of diffusion (model C). As an important result, solute profiles alone are a poor indicator of tubificid tracer
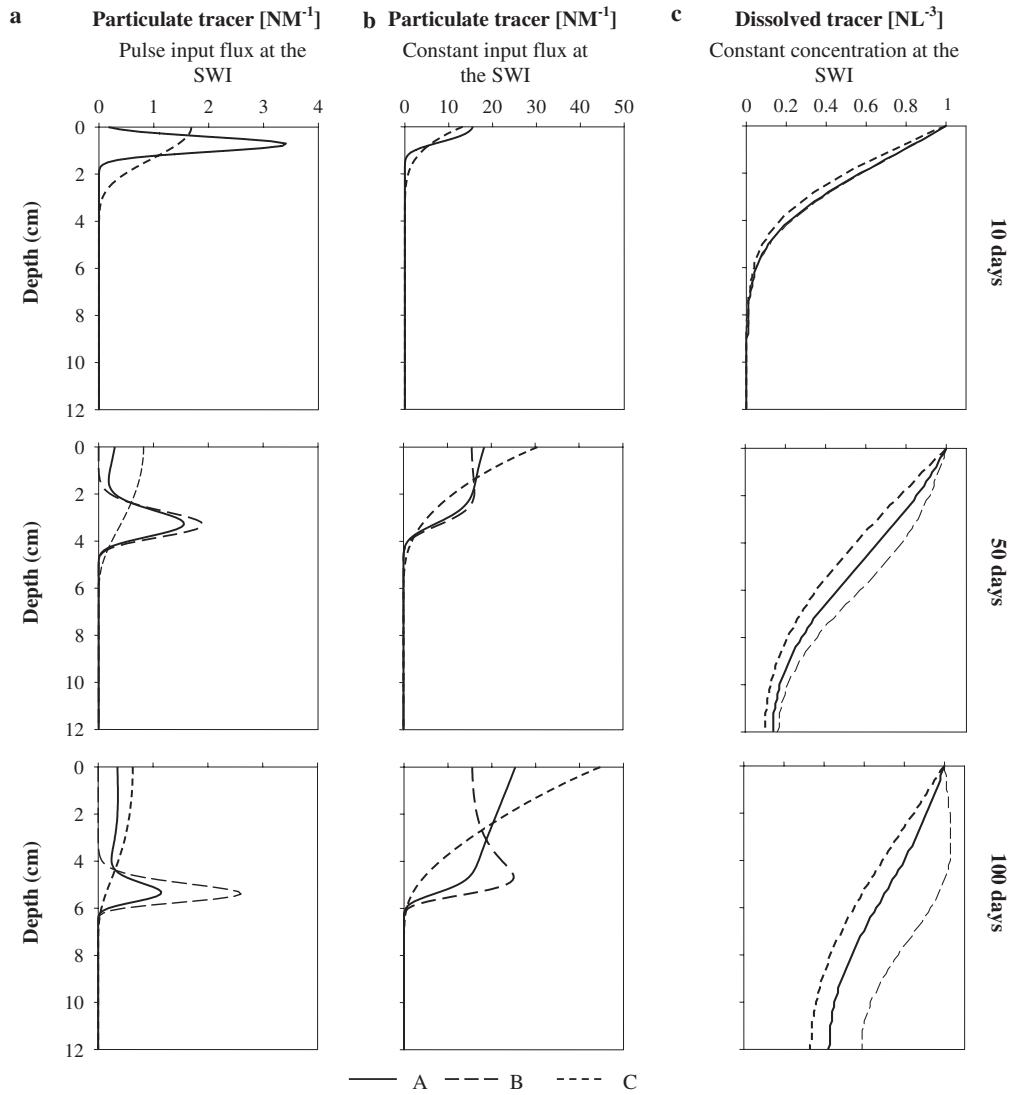
Fig. 2. Sensitivity analysis of tubificid bioturbation mechanisms. Three simplified models were used to simulate a conservative tracer ($R_s = R_f = 0$). Model A incorporates all three transport mechanisms (ingestion, bioadvection, and biodiffusion). Model B reduces to a simple advection-diffusion model. Model C only retains biodiffusive mixing. (a) Scenario 1: input pulse of solid tracer at the SWI. (b) Scenario 2: constant input flux of solid tracer at the SWI. (c) Scenario 3: flux of solute tracer with constant concentration in the overlying water. Parameters values are given in Table 1. At 10 days, the tracer profiles generated by models A and B cannot be distinguished from each other.

transport, and hence, one needs to analyse solid tracer profiles to properly constrain biological transport parameters.

4.2. Model calibration: microsphere transport

A first remarkable observation is that the calibrated biological transport parameters are nearly similar for all four datasets analysed (two treatments with each two replicates) (Table 2), even if k_{ing}^{max} is higher in the replicate a of the $\{-Cd + Tub\}$ condition. The fact that replicates provide similar parameter values is not surprising, since the data profiles of the replicates are very similar for both treatments. More remarkable is that biological transport parameters attain similar values for the $\{-Cd + Tub\}$ and $\{+Cd + Tub\}$ treatments. Therefore, cadmium contamination seems not to affect tubificid bioturbation.

Table 2
Transport parameters values obtained from the calibration step on microspheres profiles

Dataset	D_b^0 (cm^2 yr^{-1})	k_{ing}^{max} (yr^{-1})	x_{ing} (cm)	SQE
$\{+Cd + Tub\}$a	2.7	12.6	5	0.32
$\{+Cd + Tub\}$b	3.1	11.7	5	0.28
$\{-Cd + Tub\}$a	3.3	16.6	5	0.31
$\{-Cd + Tub\}$b	3	12.4	5	0.28

For each condition and each replicate, a set of values for the free transport parameters was calibrated to minimize the cost function represented by the SQE (sum of squared error between simulated and measured profiles).

Hence, an average set of values can be obtained from these four simulation runs: the mixing rate $D_b^0 = 3$ cm^2 yr^{-1}, the ingestion rate $k_{ing}^{max} = 13.3$ yr^{-1} and the ingestion depth $x_{ing} = 5$ cm. With these values, a simulation was ran and

the output was compared to the microspheres profiles (Fig. 3). The simulation output shows a good agreement with the microsphere data. In both the {−Cd + Tub} and {+Cd + Tub} treatments, the two replicate experiments show a very similar and characteristic pattern. The transient data profiles show very similar features as those that were noted in the sensitivity analysis of the previous section (model A response to input pulse, Fig. 2a): (i) a gradual peak broadening when the pulse is buried deeper into the sediment, (ii) the disappearance of the pulse when reaching the ingestion depth, and (iii) the homogenization of the sediment layer above the ingestion depth. This indicates that our model captures the relevant aspects of tubificid bioturbation (ingestion/deposition, bioadvection, and diffusive mixing). The simulation output produces though a more ''pronounced'' response with higher peaks than the data. The correspondence between simulations and data is hampered by the averaging that results from low-resolution core slicing. This is particularly true for the deeper layer, where the sediment between 5–12 cm was pooled
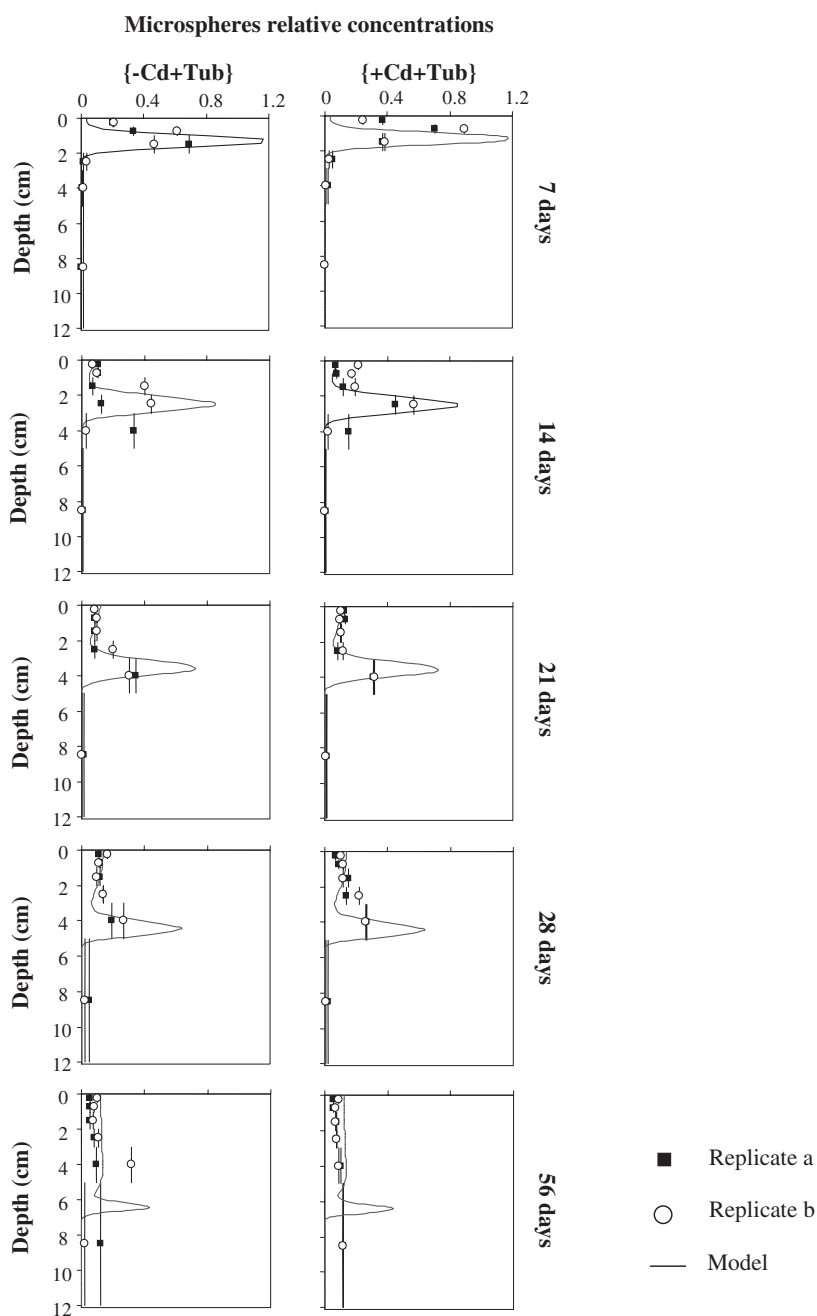

Fig. 3. Comparison of: (i) a simulation of conveying-belt transport that was run with transport coefficients averaged over the whole of the values from calibration step (Table 2); (ii) microspheres profiles in two different treatments (with two replicates each). Parameters values are given in Table 1. The model profiles show good agreement with the experimental data except at 56 days. Vertical bars denote the thickness of the sediment slices that were used to obtain the data.

together. To enable a proper comparison, one can also average the simulation output over the corresponding sediment slices, and these profiles show a good agreement with the data (results not shown). Our model simulations lead to two important observations. Firstly, biological transport parameters were kept constant during the simulations, assuming that biological activity remains unchanged during the experiment. This assumption seemed to work out well, but for the last period between 28 and 56 days. At 56 days the tracer inventory above the ingestion depth is over predicted, indicating that too many microspheres are brought upwards by ingestion. The large thickness of the deepest sediment layer (5–12 cm) prohibited a more precise tuning of the model's response at depth. Secondly, the application of the conveyor-belt model provides quantitative biological information about tubificid ingestion: the advective velocity at $x = 0$ induced by ingestion/egestion is about 66 cm yr^{-1}, corresponding to a flux of egested sediment of 43 g dry sediment cm^{-2} yr^{-1}. Using a density of 60,000 individuals per m^2, one thus obtains an egestion rate of 7 g per individual per year. Using a value of 0.7 mg dry weight per individual (measured for *Tubifex tubifex*; Guerin, 1994), this gives an egestion of 10 g dry sediment per mg dry weight of worm per year.

4.3. Model application: cadmium biogeochemistry

The simulation of cadmium profiles was carried out with the same values of the biological parameters as constrained from the microsphere profiles (Table 1). Results for the {+Cd + Tub} treatment are presented in Fig. 4. Our model simulations provide values for the four components that control the cadmium exchange across the SWI: the external dissolved flux F_f^{ext}, the external particulate flux F_s^{ext} and the tubificid egestion fluxes F_f^b and F_s^b (Table 3). This shows that 25–50% of the "new" cadmium entering the sediment is of the solute form, and therefore, the external solid input F_s^{ext} represents 50–75% of total exchange F_{tot}^{ext}. The flux F_s^b of particulate cadmium due to deposit-feeding ranges from about 20% to 50% of the new input F_{tot}^{net}. The dissolved flux F_f^b due to deposit-feeding is negligible.

Model output and data show good agreement up to 21 days both for particulate and dissolved cadmium profiles. The profiles of dissolved cadmium have a conspicuous shape. Within the first millimetre, the concentration decreases strongly. Deeper however, the dissolved profile adopts the same shape as particulate profile. This discontinuity can be explained by the relative rate of transport and reactive processes. Within the first millimetre, molecular diffusion is fast and is able to keep the cadmium adsorption out of equilibrium. Below the first millimetre, the fast sorption process (80 yr^{-1}) dominates, and consequently, both solid and solute profiles are near sorption equilibrium. This implies that but for the first mm, the two principal processes determining the observed cadmium profiles are the (i) the biological down-mixing of solid cadmium by

tubificids, and (ii) the subsequent redistribution of cadmium between solid and liquid phases via sorption.

At 56 days, the simulated cadmium profiles do not fit the measured profiles. The simulations predict a higher transfer of cadmium to depth than in is observed in the data. Two hypotheses can be proposed for a change before and after the 21 days sampling point: (i) a change in cadmium sorption resulting from a switch in redox geochemistry; (ii) a change in biological activity affecting biological transport parameters. The oxygen and manganese data, presented in Ciutat et al. (2005b), provide no evidence for a temporal change in the redox conditions of the sediment during this period: neither the overall re-oxidation rate changes (as indicated by the oxygen penetration depth) nor one can detect a change in the suboxic geochemistry (as indicated by steady profiles of the pore water manganese). Moreover, the cadmium data at 7 and 21 days do not show a different partitioning between solid and liquid phase when compared to those at 56 days (no outlier in the regression of Fig. 1), and hence, there is no evidence for a temporal change in the partitioning coefficient). Accordingly, the first hypothesis seems invalid. The second hypothesis is however not in contradiction with the microsphere results. Despite the considerable uncertainty about the deepest layer in the microsphere simulations, the profile at 56 days already hinted at a decreased biological activity in the period from 28 to 56 days. Moreover, the simulations of the microspheres show higher concentrations from the surface to the subsurface peak than the measured profiles, which could be attributed to a decrease of the ingestion/egestion processes. To test this hypothesis, we carried out an additional simulation, where we fixed k_{ing}^{max} at the value of 13.3 yr^{-1} for the first 28 days, and reduced it to 3 yr^{-1} between 28 and 56 days. Resulting profiles are presented in Fig. 5. The agreement with the microspheres data slightly improves: particularly, tracer concentrations from surface to subsurface peak are better represented than in the previous simulations of Fig. 3. However, the agreement with experimental cadmium profiles improves significantly, and hence, a decrease of tubificid ingestion rate after 28 days seems the most plausible explanation for the observed cadmium distribution at 56 days.

5. Discussion

5.1. Tubificid bioturbation: parameter calibration and model complexity

5.1.1. Parameter calibration strategy

The biogeochemical model explored here simulates the concentration evolution of two solid tracers and one dissolved tracer, and incorporates fourteen parameters in total: (i) three parameters specifying the sediment environment (φ, ρ_s, T); (ii) five parameters determining the biological transport (D_b^0, x_{mix}, k_{ing}^{max}, x_{ing}, and σ_{ing}); (iii) two parameters determining cadmium sorption (K_p and k_{ad}); (iv) the diffusivity of dissolved cadmium D_0; (v) three
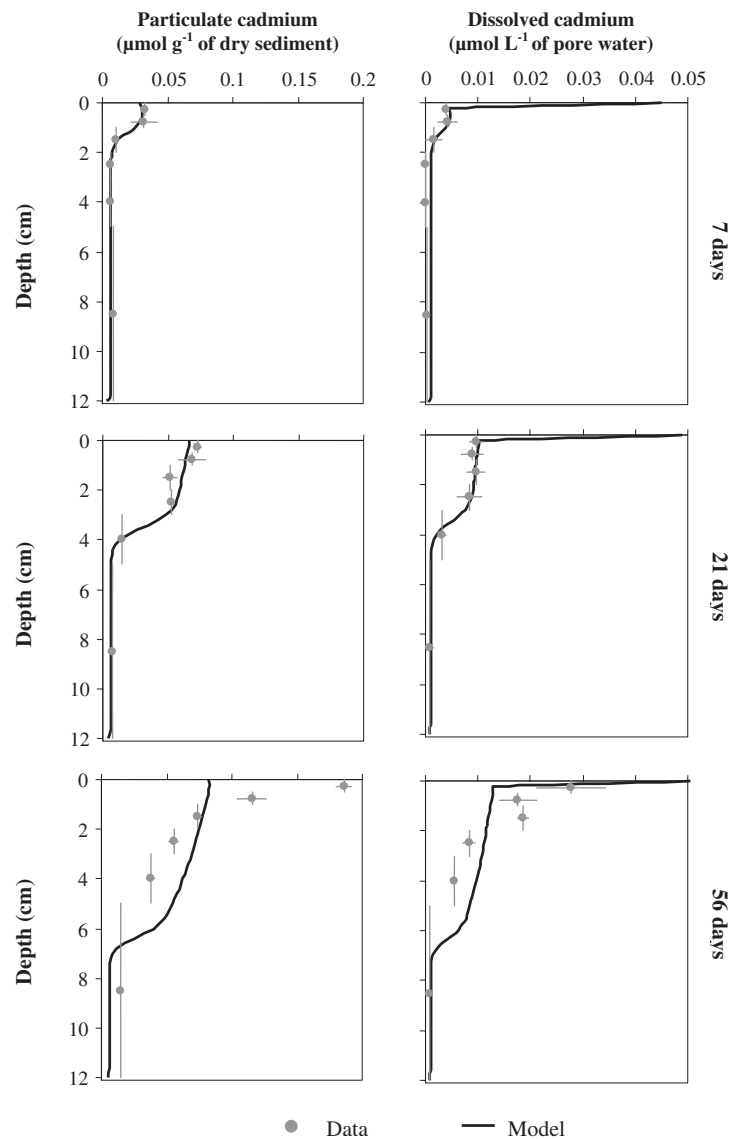
Fig. 4. With the values of transport and reaction parameters obtained from the calibration procedure (see text), the model was applied on {+Cd + Tub} cadmium profiles. Parameters values are given in Table 1. The model shows a good fit at 7 and 21 days but overestimates the cadmium transfer to depth at 56 days.

parameters describing the experimental conditions (C_f^0, $C_s(x,0)$, and $C_f(x,0)$, and F_s^{ext}). Given such a high number of degrees of freedom within the model, one needs a suitable strategy to constrain these parameters. Robbins (1986) already underlined the risk that the application of such a complex model could degenerate "into a meaningless parameter-fiddling exercise". Indeed, this would be the case, when calibrating many parameters simultaneously on a limited dataset. To avoid this pitfall, we adopted a systematic procedure, where parameters are constrained in a stepwise fashion. Five parameters were fixed *a priori* based on direct measurements: temperature, porosity, density of the solid phase, dissolved cadmium concentration in the overlying water C_f^0 and initial background concentrations of cadmium $C_s(x,0)$ and $C_f(x,0)$. In addition, the molecular diffusion coefficient D_0 for dissolved cadmium was

calculated from the temperature using a standard relation from literature. This way, eight parameters were left undetermined. This number was further reduced by using literature values for the mixing depth x_{mix} and the spreading σ_{ing} of the ingestion depth. The remaining six parameters were calibrated using experimental data from the incubations, and this was done in a sequential fashion.

In a first step, the two reaction parameters K_p and k_{ad} were determined from the incubation without tubificids. Reported values for the cadmium partitioning coefficient K_p vary widely. Garnier et al. (1997) and Ciffroy et al. (2001) give values from 20 to 110 L g^{-1} for fresh water sediments. Comber et al. (1995) give values from 3 to 5 L g^{-1} for estuarine settings (values at salinity of 0). For soils (pH from 5 to 8), Allen et al. (1995) report values from 0.008 to 4 L g^{-1}. Our value of 6.44 L g^{-1} for K_p is in the order of

Table 3
The various fluxes of particulate and dissolved cadmium at the SWI (μmol cm^{-2} yr^{-1})

Days	F_s^b (Eq. (17))	F_f^b (Eq. (13))	F_s^{ext} (Eq. (19))	F_f^{ext} (Eq. (15))	F_{tot}^{net} (Model forcing)	F_{tot}^{net} (Measured by Ciutat et al., 2005b)
7 (Fig. 4)	0.31	5.5 10^{-5}	0.59	0.51	1.1	0.94 ± 0.16
21 (Fig. 4)	0.78	1.4 10^{-4}	1.71	0.49	2.2	2.04 ± 0.15
56 (Fig. 5)	0.3	5.3 10^{-5}	1.3	0.4	1.7	1.8 ± 0.1
7 (One-phase model)	0.31	0	1.1	0	1.1	0.94 ± 0.16
21 (One-phase model)	0.78	0	2.2	0	2.2	2.04 ± 0.15

F_f^b and F_s^b represents the fluxes of dissolved and particulate cadmium resulting from ingestion/egestion. F_f^{ext} represents the diffusive transfer of dissolved cadmium from the overlying water to the pore water and was calculated *a posteriori* from the resulting profiles. F_s^{ext} represents the input of particulate cadmium for overlying water to the sediment, which was used as a forcing function in the model. F_s^{ext} was deduced from the imposed value of at F_{tot}^{net} each time step using equation. (19). Simulated and measured values of the total flux F_{tot}^{net} across the SWI in the {+Cd + Tub} treatment are also presented.

these reported literature values. No reported values for k_{ad} were found but Garnier et al. (1997) and Ciffroy et al. (2001) showed a rapid sorption kinetic for cadmium (on the order of hours). The value for k_{ad} obtained in this study (80 yr^{-1}) confirms rapid sorption equilibrium (yet on the order of days rather than hours).

In a second step, the inert microspheres profiles from the {−Cd + Tub} and {+Cd + Tub} were used to constrain the three free biological parameters D_b^0, k_{ing}^{max} and x_{ing} (determining three parameters from 120 data points, i.e., 20 profiles containing 6 data points each). This way, the final "application" simulation of the {+Cd + Tub} incubation only involved one free parameter, i.e., the external flux F_s^{ext} of cadmium to the sediment.

Our strategy for calibrating parameters differs from other modelling treatments of conveyor-belt transport. A dual tracer approach is adopted, where biological transport parameters are first calibrated on a "training tracer" (the microspheres profiles) and subsequently applied on an independent "application tracer" (the cadmium profiles). In previous model investigations of conveyor-belt bioturbation, a single tracer was used: [137]Cs in Fisher et al. (1980); [7]Be in Rice (1986); ^{137}Cs in Robbins (1986); ^{137}Cs and ^{210}Pb in Christensen and Bhunia (1986); ^{51}Cr in Timmermann et al. (2003). In these, biological transport parameters are calibrated without a second independent test. Mohanty et al. (1998) and Reible and Mohanty (2002) applied their models on pyrene profiles but used direct independent measurements of the ingestion rate.

5.1.2. Tubificid bioturbation

The tubificid model includes two modes of transport. (i) Small-scale diffusive mixing. This transport presumably results from burrow construction, movement in and out of burrows, and the dragging of particles within burrow galleries (Robbins, 1986), and is modelled by two parameters: D_b^0 and x_{mix}. (ii) Nonlocal transport. This long-range transport (several centimetres) results from ingestion/egestion, and is modelled by three parameters: k_{ing}^{max}, x_{ing} and σ_{ing}. The parameter values obtained here can be compared to other studies on tubificid bioturbation (Table 4). Our value of 3 cm^2 yr^{-1} for the biodiffusion coefficient compares very well with other modelling studies of tubificid bioturbation that explicitly include a conveyor-belt mechanism in addition to a biodiffusion term: 0.73 cm^2 yr^{-1} (Robbins, 1986), 2.7 cm^2 yr^{-1} (Fisher et al., 1980), 2.5–3.1 cm^2 yr^{-1} (Ciutat et al., 2005a). Note that these are rather low mixing intensities, given the high densities of organisms involved (10^4–10^5 ind m^{-2}). Modelling studies that describe tubificid particle transport exclusively via a biodiffusive mechanism do find considerably higher mixing coefficients: 0.9–8.5 cm^2 yr^{-1} (Christensen and Bhunia, 1986), and 0.5–23 cm^2 yr^{-1} (Reible et al., 1996). Clearly, in these latter studies, the transport due to conveyor-belt mechanism is "disguised" as biodiffusive mixing, thus leading to significantly higher biodiffusion values.
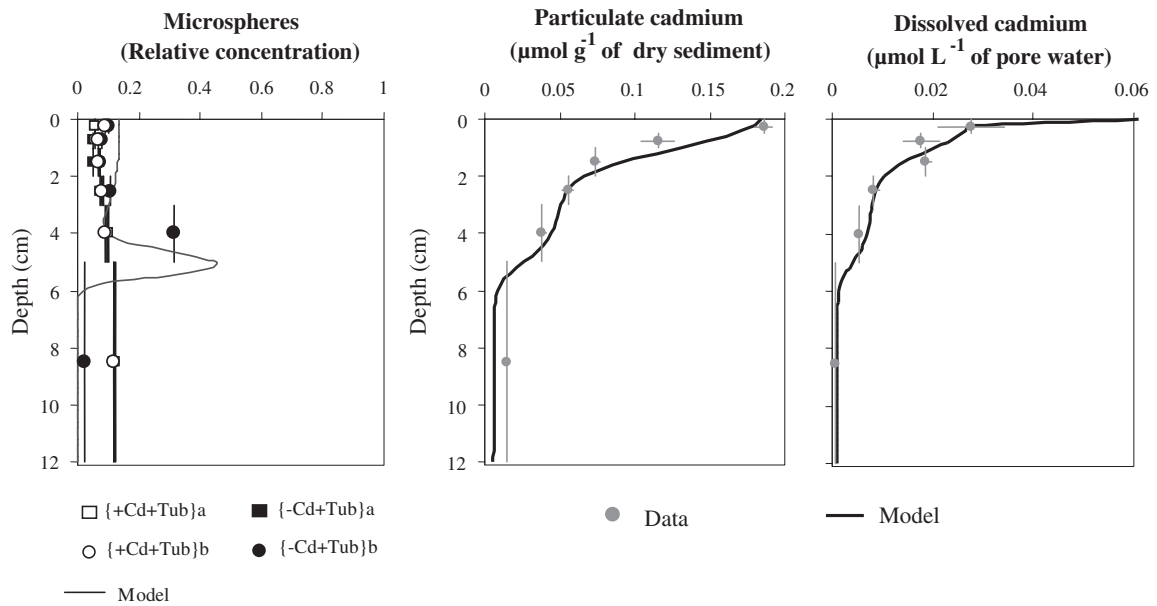
Fig. 5. Test simulation to investigate the effect of a decrease in tubificid activity after 28 days. The model was ran with a value of $k_{\text{ing}}^{\text{max}} = 13.3$ yr^{-1} from 0 to 28 days and with a lower value of $k_{\text{ing}}^{\text{max}} = 3$ yr^{-1} between 28 and 56 days. In these two simulations, the others transport parameters were fixed to the values given in Table 1.

Past modelling studies on tubificids use different formulations for the depth-dependency of biodiffusion. Robbins (1986) used the same mathematical representation (4) as here, and gave values from 1.5 to 2 cm for the characteristic mixing depth x_{mix}. In their exclusively biodiffusive model, Christensen and Bhunia (1986) used values from 0.45 to 1.8 cm for x_{mix}. Robbins et al. (1977) represented biodiffusion as constant from surface to a certain mixing depth, whereafter mixing suddenly vanishes. They found values from 3 to 6 cm for the depth of the mixed zone. Note that in the formulation (4), the characteristic mixing depth x_{mix} may be interpreted as the square root variance of a Gaussian distribution. Accordingly, "cutting" the mixed zone at two or three times the variance, the values of Robbins et al. (1977) conform to the $x_{\text{mix}} = 2$ value used here.

An ingestion rate of 10 g dry sediment per microgram dry weight of worm per year was calculated (see Section 4). This compares well with the value of 6 g calculated by Appleby and Brinkhurst (1970) from measured defecation rates, but is higher than the 1.3 g reported by Reible et al. (1996). In our study, the inherent bioadvective velocity was calibrated to 66 cm yr^{-1}, which is in the highly variable range of 3–600 cm yr^{-1} reported in the literature (Table 4). As noted by Fisher et al. (1980), tubificid activity is dependent on a number of biotic factors (intrinsic characteristics of studied population, biotic interactions) and abiotic factors (temperature, chemical conditions). Moreover, experimental or modelling techniques used to quantify the transport parameters are variable. Accordingly, the comparison of the results from different studies remains difficult.

The depth of maximal ingestion x_{ing} was set to 5 cm, which is close to the value of 6–7 cm obtained by Ciutat

et al. (2006) using X-rays. Our value is also in accord with the interval of 5–7 cm given by Fisher et al. (1980), and with the depth of 4 cm given by Davis (1974) and Robbins (1986). The variance of ingestion zone σ_{ing} was set to 2 cm following Robbins (1986) who gave values from 1.5 to 2 cm. This value is higher than the value of 0.5 cm given by Fisher et al. (1980), but this difference is probably due to the different formulation of the depth dependent ingestion.

Despite some unavoidable variation, this compilation of model parameters displays a great consistency between studies. This is quite remarkable, as these experimental studies differ in a numbers of ways: different tracers, different tubificid species and different environmental conditions. Accordingly, this opens perspectives with regard to the use of models as predictive tools in contaminant risk analysis in freshwater sediments. A crucial problem in such risk analysis is to find parameter values that are suitable for the conditions at hand. As indicated by the above review, tubificid parameters are quite narrowly constrained across different environments, and hence, it seems possible to construct derive a "generic" tubificid bioturbation model (e.g., $D_b^0 \approx 3$ cm^2 yr^{-1}; $x_{\text{mix}} \approx 2$ cm; $k_{\text{ing}}^{\text{max}} \approx 10$ yr^{-1}; $x_{\text{ing}} \approx 5$ cm; $\sigma_{\text{ing}} \approx 1$ cm). Such a generic model could be useful to run specific scenarios for certain contaminants, and get a ball park idea about the accumulation and/or removal of these contaminants from the sediment environment.

5.1.3. Model complexity

The present model employs five parameters (D_b^0, x_{mix}, $k_{\text{ing}}^{\text{max}}$, x_{ing} and σ_{ing}) to describe conveyor-belt bioturbation by tubificids. Apparently, this conveyor-belt model captures tubificid bioturbation rather well, as suggested by the good agreement between model profiles and data.

Table 4
Reported values from literature on tubificid bioturbation rates

	Species	Densities (ind m^{-2})	Temperature (°C)	Transport model	D_b^0	K_{ing}^{max}	x_{mix}	ω_b	x_{ing}	σ_{ing}	Tracer
Davis (1974)	*Linnodrillus sp.*	800–1800	8–10	Conveying-belt				3.1	3–4		^{137}Cs
In Fisher et al. (1980)	*Linnodrillus hoffmeisteri* *Linnodrillus udekemianus*	100,000	20–22	Conveying-belt Conveying-belt				84–609 99–591			
	Tubifex tubifex			Conveying-belt	2.7			37–124	5–7	0.5	^{210}Pb, ^{137}Cs
Christensen and Bhunia (1986)	*Linnodrillus hoffmeisteri*	630–5700	4–6	Biodiffusion	0.9–8.5		0.45–1.8				
Robbins (1986)	*Tubifex tubifex Linnodrillus hoffmeisteri*	50,000	20–22	Conveying-belt	0.73	5.11	1.5–2	20	4	1.5–2	^{137}Cs
Reible et al. (1996)	*Tubifex tubifex Linnodrillus hoffmeisteri*	6700–26700		Biodiffusion and ingestion	0.5–23						Pyrene
Ciutat et al. (2006)	*Tubifex tubifex Linnodrillus hoffmeisteri*	60,000	20	Conveying-belt					6–7		X-rays granulometry
Ciutat et al. (2005a)	*Tubifex tubifexLinnodrillus hoffmeisteri*	60,000	20	Conveying-belt	2.5–3.1			55–105			Luminophores (63–100μm)
Our study	*Tubifex tubifex Linnodrillus hoffmeisteri*	60,000	20	Conveying-belt	3	13.3		66	5	2	Microspheres (1μm)

Experimental conditions are presented (organism densities, temperature and tracer). Different studies used different models and different parameterisations to quantify bioturbation: the dominant transport mode incorporated to model the bioturbation is indicated each time. As a result of model variation, the values of single parameter may greatly vary between studies.

However, the question arises whether this complexity is really appropriate (Soetaert et al., 1996; Andersson et al., 2006; Meysman et al., 2006b)? In other words, would a more complex model (with an increased number of parameters) enable a better fit, or oppositely, is it possible to reduce the complexity of the present model and still keep a good agreement with data. This point is of critical importance when transposing the modelling approach from small-scale lab experiments to large-scale field applications. For example, coupled benthic-pelagic ecosystem models are limited in the complexity by which the sediment compartment is described.

Three relevant questions can be investigated: (i) Is it really needed to explicitly model the dissolved cadmium phase? (ii) How important is small-scale mixing in tubificid bioturbation? (iii) Is a conveyor-belt model really needed, or is a simple biodiffusive model sufficient to model the cadmium diagenesis? These three points were tested with simplified versions of the tubificid transport model and the results are presented in Figs. 6 and 7.

5.1.3.1. Relevance of the dissolved phase. Simulations at 7 and 21 days were performed using only Equation (1) for particulate cadmium with the reaction term set to zero. Biological transport parameters were given exactly the same values as in two-phase cadmium model simulations. To compensate for the dissolved flux F_f^{ext}, the external solid flux F_s^{ext} was increased to 1.1 and 2.2 μmol cm^{-2} yr^{-1} respectively at 7 and 21 days. The concentration profiles obtained from this one-phase cadmium simulation are nearly identical to the ones obtained by the two-phase model (results not shown). Accordingly, the solute phase is not needed when applying the tubificid model on cadmium data. Tubificid bioturbation determines the solid phase cadmium distribution, and the fast sorption process then completely determines the solute distribution. This also justifies our initial assumption that the influence of bioirrigation is small. The one-phase model has definitely an advantage when a simplified modelling approach is required, as often is the case when developing water quality models or in whole ecosystem approaches. Still, the two-phase model is more informative about the nature of the fluxes, and the contribution of each phase to the global behaviour of cadmium in sediment. Nevertheless, one should be cautious when applying the model to other metals and other environments with other bioturbating fauna. The dissolved phase can only be neglected when sorption strongly favours the adsorption of the metal on the particulate phase, and when bioturbators do not irrigate their burrows.

5.1.3.2. Importance of biodiffusion as a tubificids transport mode. To investigate the sensitivity of the solid cadmium profiles to small-scale mixing, we decreased the biodiffusion coefficient and compared simulations with $D_b^0 = 0.03$, 0.3, and 3 cm^2 yr^{-1} (Fig. 6). The differences between the simulated profiles are minor. When $D_b^0 = 3$ cm^2 yr^{-1} one

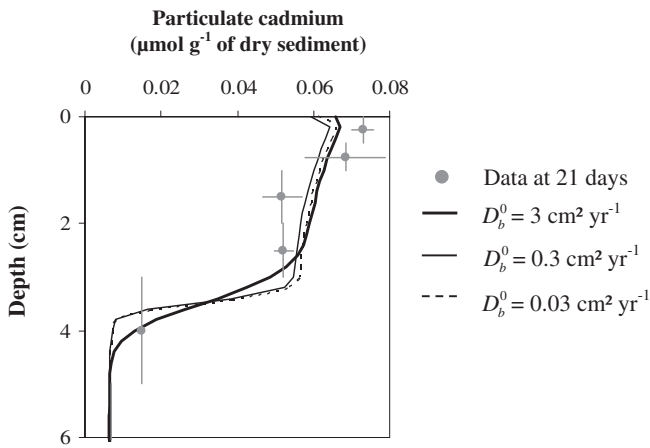**Fig. 6.** Test simulation to investigate the influence of the biodiffusion on cadmium dispersal. Application with $D_b^0 = 0.03$, 0.3, and 3 cm^2 yr^{-1}. Other parameters are fixed to their baseline values given in Table 1. Biodiffusion is a negligible process in the transport of cadmium by tubificid bioturbation.

observes a certain "smoothing" of the concentration profile, particularly around the ingestion depth. However overall, the small-scale mixing does not seem to be a critical aspect of the transport induced by tubificid conveyor-belt feeders. A similar conclusion was reached by Rice (1986) for the Polychaete *Scoloplos* spp.

5.1.3.3. The biodiffusive approach. The biodiffusion model is the standard representation of bioturbation in biogeochemical models of aquatic sediments (e.g., Rabouille and Gaillard, 1991; Wijsman et al., 2002; Meysman et al., 2003). Accordingly, one can ask whether the biodiffusion model could not be used to interpret the present dataset. To test this, we performed simulations of the particulate cadmium with only biodiffusive mixing, while calibrating the biodiffusion coefficient D_b^0 at the sediment surface, but retaining $x_{mix} = 2$ cm. An external solid flux F_s^{ext} of 1.1,

2.2, and 1.7 μmol cm^{-2} yr^{-1} was imposed at 7, 21 and 56 days, respectively. For a D_b^0 value of 50 cm^2 yr^{-1}, the model provides a reasonable fit to the data (Fig. 7), particularly at 7 and 56 days. At 21 days, there is a considerable overprediction of tracer in the surface layer. At 56 days, the fit is better, though the model still overpredicts the concentration in the 1–3 cm depth layer, and underpredicts it from 5 cm downwards. Apparently, there is a clear time-scale aspect involved. Cadmium profiles exhibit a shape that is typical of conveyor-belt mechanism at 7 and 21 days, but turn to a biodiffusive shape at 56 days. Over short time-scales, the conveyor-belt model seems to have an edge over the biodiffusion model, as the conveyor-belt model captures the actual mechanism of tubificid bioturbation. However, as the time-scale of observation increases, tubificid bioturbation looks more and more "diffusive", and so the simple biodiffusion model (two parameters) becomes more and more of an alternative to the conveyor-belt model (three parameters). This agrees with the theoretical prediction that the biodiffusive model is appropriate for tracer modelling at a long term scales, but may show considerable bias at short time-scales (Boudreau, 1986a; Meysman et al., 2003). One should note that short time-scales are typical for contamination experiments like the incubations analysed here. For these, the biodiffusion model provides little advantage, due to its mechanistic deficit. A biodiffusive approach would not permit to detect the change in the biological activity between 28 and 56 days, as tentatively observed here. Therefore, when using bioturbation as a bioindicator of pollutant effects or environmental changes, the conveyor-belt model could be a more efficient tool to detect changes in biological activity.

5.2. Tubificid bioturbation under cadmium contamination

A remarkable result is that there is no difference in the calibrated biological transport parameters between the {−Cd + Tub} and {+Cd + Tub} treatments: tubificid
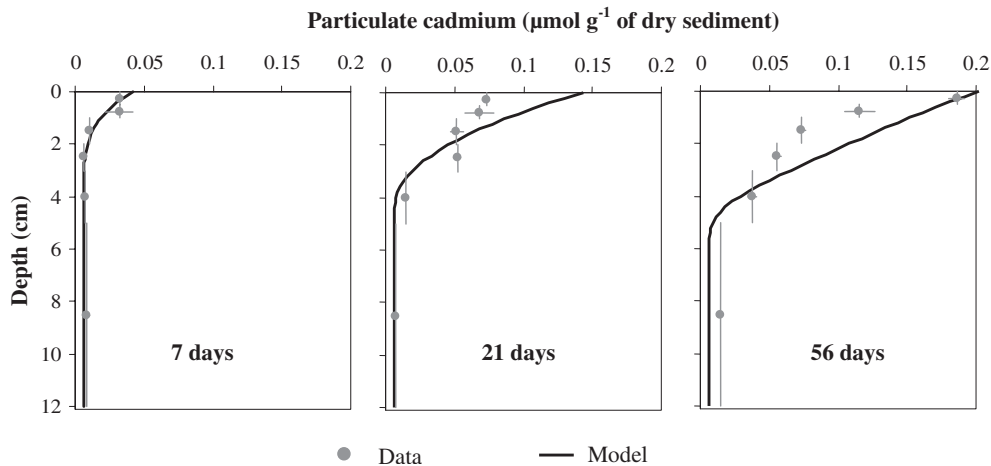

Fig. 7. Application of a simple biodiffusive model that only accounts for the particulate phase of cadmium. Value of D_b^0 was set to 50 cm^2 yr^{-1}. Other parameter values are given in Table 1. The biodiffusive model gives a proper fit at 7 and 56 days, but not at 21 days.

bioturbation appears not to be affected by cadmium contamination. This confirms the conclusions of Ciutat et al. (2005a) who proposed that strong detoxification be at work in tubificids. Several authors have reported a tolerance to high contamination level of metals in oligochaetes. This tolerance can be due to several detoxification mechanisms: (i) intracellular compartmentalization involving lysosomes, spherocrystals or metal containing granules (Brown, 1982; Dhainaut-Courtois et al., 1998); (ii) metal inactivation by binding to metallothionein-like proteins (Wallace et al., 1998; Gillis et al., 2002); (iii) sequestration in sulphur-rich granules located in chloragocytes, body wall and gut wall cells (Klerks and Bartholomew, 1991).

5.3. Cadmium behaviour under tubificids bioturbation

The cadmium biogeochemistry in aquatic sediments is complex, and the conveyor-belt mechanism of tubificids interacts with this chemistry in a complex way. Ciutat et al. (2005b) provide a discussion about cadmium biogeochemistry in the experiments presented here. Tubificids do not modify the oxygen penetration depth within the sediment. Oxygen is rapidly consumed in the first 3–5 mm due to aerobic respiration, and re-oxidation of reduced compounds. McCall and Fisher (1980) reported enhanced oxygen consumption compared to the simple sum of worm metabolism and bacterial respiration in control sediment. They attributed this difference to the oxidation of FeS transferred to the surface by conveyor-belt transport and to enhanced microbial activity. Tubificid transport also modifies the cycling manganese (and possibly iron) within the sediment, homogenizing the distribution of particulate manganese and enhancing manganese re-oxidation near the surface (Ciutat et al., 2005b). Petersen et al. (1998) suggested that the higher transport of cadmium from the water column into bioturbated sediments is driven in part by adsorption onto these metal oxides (iron and manganese). Cadmium is trapped within in the first millimetres of sediment on manganese and iron oxides, which are then transferred to depth via bioadvection.

Our model does not account for such complex chemistry interactions, primarily because the geochemical data (e.g., the iron oxide distribution) are lacking that could validate such a complex diagenetic model formulation. Instead, the model includes simple sorption kinetics to describe the partitioning of cadmium between solute and solid phase. Despite its simplicity, this approach seems to capture the dominant aspects that govern the fate of cadmium in freshwater sediments. The partitioning coefficient K_p is high, and strongly favours the sorption of cadmium onto the particle phase of the sediment. Without tubificids, sorption processes prevent the migration of cadmium at depth because the dissolved cadmium from overlying water remains "trapped" near at the surface in a particulate form. With tubificids, this particu-

late material is rapidly buried due to the bioadvective effect resulting from deposit-feeding, and accordingly, it becomes deeply distributed. To reach a depth of 5 cm, cadmium needs about 30 days under tubificid bioturbation. The same penetration would require more than 20 years without tubificids. This difference in time scale indicates the critical importance of biological transport, and more particularly conveyor-belt processes (see Fig. 6) for cadmium transport to deep sediment. At depth, the adsorbed cadmium is again desorbed to satisfy the partitioning equilibrium. This explains the similar shape of particulate and dissolved cadmium profiles below the first millimetre. This role of tubificid in transport of metals was already put forward by Soster et al. (1992) who concluded that the higher level of Zn found in the upper 3 cm of tubificid-inhabited sediments was probably caused by bioadvective particle movement and adsorption, rather than by solute diffusion.

6. Conclusion

Freshwater sediment is inhabited by tubificids (Oligochaeta), and this taxon becomes predominant when the system is human-impacted. Consequently, tubificids exert a great control on the fluxes of contaminants across the SWI. Conveyor-belt transport was investigated and modelled by several authors during the two last decades. However, it was not included into multi-components reactive models, where biodiffusion remains the standard description of bioturbation.

This case study of tubificid bioturbation clearly shows the advantages of including a more mechanistic description of deposit-feeding into a diagenetic model: (i) it provides far more accurate description of solid tracer transfer to depth, particularly at short time-scales, when compared to biodiffusion models; (ii) it enables a precise quantification of the various transport rates (ingestion, bioadvection, and biodiffusion), and this way, it allows the estimation of important biological characteristics (e.g., mixing depth, ingestion rate of deposit-feeders)); (iii) it sheds a light on the fate and transport of a contaminant (in this case cadmium) under tubificid bioturbation. The application of the model clearly provided insights and allowed the estimation of processes rates that cannot be directly deduced from data. Particularly, we showed that the solute phase needs not to be accounted for when: (i) the sorption equilibrium establishes fast and is strongly in favour of the solid phase; and (ii) bioirrigation is not an important transport mechanism. In this case, particle transport governs the fluxes at the SWI and the redistribution of contaminant into the sediments.

Based on a comparison with past studies, we propose a generic model of tubificid bioturbation that could be used to predict contaminant dispersal in various sedimentary environments. Clearly, this model needs to be tested on field data to assess its accuracy in natural environments with tracers other than cadmium.

Associate editor: Chen Zhu

References

Allen, H.E., Chen, Y.T., Li, Y.M., Huang, C.P., Sanders, P.F., 1995. Soil partition coefficients for Cd by column desorption and comparison to batch adsorption measurements. *Env. Sci. Technol.* **29**, 1887–1891.

Andersson, J.H., Middelburg, J.J., Soetaert, K., 2006. Identifiability and uncertainty analysis of bio-irrigation rates. *J. Mar. Res.* **23**, 407–429.

Appleby, A.G., Brinkhurst, R.O., 1970. Defecation rate of three tubificid oligochaetes found in the sediments of Toronto Harbour, Ontario. *J. Fish. Res. Bd. Can.* **27**, 1971–1982.

Banta, G.T., Andersen, O., 2003. Bioturbation and the fate of sediment pollutants. *Vie Milieu* **53**, 233–248.

Berner, R.A., 1980. *Early Diagenesis, A Theoretical Approach. Princeton Series in Geochemistry*. Princeton University Press, New Jersey.

Boudreau, B.P., 1986a. Mathematics of tracer mixing in sediments: I. Spatially-dependent, diffusive mixing. *Amer. J. of Sci.* **286**, 161–198.

Boudreau, B.P., 1986b. Mathematics of tracer mixing in sediments: II. Nonlocal mixing and biological conveyor-belt phenomena. *Amer. J. of Sci.* **286**, 199–238.

Boudreau, B.P., 1997. *Diagenetic Models and Their Implementation*. Springer, Berlin.

Brown, B.E., 1982. The form and function of metal-containing granules in invertebrates tissues. *Biol. Rev.* **57**, 621–667.

Ciffroy, P., Garnier, J.M., 2001. Mai Khanh Pham Kinetics of the adsorption and desorption of radionuclides of Co, Mn, Cs, Fe, Ag and Cd in freshwater systems: experimental and modelling approaches. *J. Environ. Radio* **55**, 71–91.

Ciutat, A., Gerino, M., Mesmer-Dudons, N., Anschutz, P., Boudou, A., 2005a. Cadmium bioaccumulation in Tubificidae from the overlying water source and effects on bioturbation. *Ecotoxicol. Environ. Safety* **60**, 237–246.

Ciutat, A., Anschutz, P., Gerino, M., Boudou, A., 2005b. Effects of bioturbation on cadmium transfer and distribution into freshwater sediments. *Environ. Toxicol. Chem.* **24**, 1048–1058.

Ciutat, A., Weber, O., Gerino, M., Boudou, A., 2006. Stratigraphic effects of tubificids in freshwater sediments: a kinetic study based on X-ray images and grain-size analysis. *Acta Oecol.* **30**, 228–237.

Christensen, E.R., Bhunia, P.K., 1986. Modeling radiotracers in sediments: comparison with observations in lakes Huron and Michigan. *J. Geophys. Res.* **91**, 8559–8571.

Comber, S.D.W., Gunn, A.M., Whalley, C., 1995. Comparison of the partitioning of trace metals in the Humber and Mersey Estuaries. *Mar. Bull. Poll.* **30**, 851–860.

Crank, J., 1976. *The mathematics of diffusion 1-Diffusion-mathematical models*, second ed. Oxford University Press, England.

Davis, R.B., 1974. Stratigraphic effects of tubificids in profundal lake sediments. *Limno. Oceanogr.* **19**, 466–488.

Dhainaut-Courtois, N., Arrouijal, F.Z., Demuynck, S., 1998. Effets biologiques de trois métaux lourds (chrome, nickel et plomb) sur Nereis diversicolor (Annélide polychète). *Oceanis* **14**, 423–433.

Fisher, J.B., Lick, W.J., McCall, P.L., Robbins, J.A., 1980. Vertical mixing of lake sediments by tubificid oligochaetes. *J. Geophys. Res.* **85**, 3997–4006.

Fu, G., Allen, H.E., 1992. Cadmium adsorption by oxic sediment. *Wat. Res.* **26**, 225–233.

Garnier, J.M., Ciffroy, P., Martin, J.M., 1997. Mai Khanh Pham Kinetics of trace element complexation with suspended matter and with filterable ligands in freshwater. *Environ. Sci. Technol.* **31**, 1597–1606.

Gillis, P.L., Diener, L.C., Reynoldson, T.B., Dixon, D.G., 2002. Cadmium-induced production of a metallothionein like protein in *Tubifex tubifex* (Oligochaeta) and *Chironomus riparius* (Diptera): correlation with reproduction and growth. *Environ. Toxicol. Chem.* **21**, 1836–1844.

Guerin, C., 1994. L'activité des Oligochètes aquatiques à l'interface eau-sédiment: Etude analytique et consequences écologqiues. Ph.D. Thesis Univ Paul Sabatier, Toulouse, France, 219 p.

Jacobs, L., Emerson, S., 1982. Trace metal solubility in an anoxic fjord. *Earth Planet. Sci. Lett.* **60**, 237–252.

Klerks, P.L., Bartholomew, P.R., 1991. Cadmium accumulation and detoxification in a Cd-resistant population of the oligochaete Limnodrillus hoddmeisteri. *Aquat. Toxicol.* **19**, 97–112.

Kresoski, J.R., Robbins, J.A., 1981. Radiotracers studies of interactions between sediments and freshwater macrobenthos. *Vehr. Int.Verein Limnol.* **21**, 382.

Kristensen, E., Kostka, J.E., 2005. Macrofaunal burrows and Irrigation in marine sediment: microbiological and biogeochemical interactions. In: Kristensen, E., Haese, R.E., Kostka, J.E. (Eds.), *Macro- and Micro-organisms in Marine Sediments*. American geophysical Union, pp. 125–157.

McCall, P.L., Fisher, J.N., 1980. Effects of tubificids oligochaetes on physical and chemical properties of Lake Erie sediments. In: Brinkhurst, R.O., Cook, D.G. (Eds.), *Aquatic Oligochaete Biology*. Plenum, New York, pp. 253–318.

Meysman, F.J.R., Boudreau, B.P., Middelburg, J.J., 2003. Relations between local, nonlocal, discrete and continuous models of bioturbation. *J. Mar. Res.* **61**, 391–410.

Meysman, F.J.R., Boudreau, B.P., Middelburg, J.J., 2005. Modeling reactive transport in sediments subject to bioturbation and compaction. *Geochim. Cosmochim. Acta* **69**, 3601–3617.

Meysman, F.J.R., Galaktionov, O.S., Gribsholt, B., Middleburg, J.J., 2006a. Bioirrigation in permeable sediments: Advective pore-water transport induced by burrow ventilation. *Limnol. Oceanogr.* **51**, 142–156.

Meysman, F.J.R., Galaktionov, O.S., Gribsholt, B., Middelburg, J., 2006b. Bio-irrigation in permeable sediments: an assessment of model complexity. *J. Mar. Res.* **64**, 589–627.

Mohanty, S., Reible, D.D., Valsaraj, K.T., Thibodeaux, L.J., 1998. A physical model for the simulation of bioturbation and its comparison to experiments with oligochaetes. *Estuaries* **21**, 255–262.

Petersen, K., Kristensen, E., Bjerregaard, P., 1998. Influence of bioturbating animals on flux of cadmium into estuarine sediment. *Mar. Environ. Res.* **45**, 403–405.

Rabouille, C., Gaillard, J.F., 1991. Towards the EDGE: Early diagenetic global explanation. A model depicting the early diagenesis of organic matter, O2, NO3, Mn, and PO4. *Geochim. Cosmochim. Acta* **55**, 2511–2525.

Rasmussen, A.D., Banta, G.T., Andersen, O., 1998. Effects of bioturbation by the lugworm *Arenicola marina* on cadmium uptake and distribution in sandy sediments. *Mar. Ecol. Prog. Ser.* **164**, 179–188.

Rasmussen, A.D., Banta, G.T., Andersen, O., 2000. Cadmium dynamics in estuarine sediments: effects of salinity and lugworm bioturbation. *Environ. Toxicol. Chem.* **19**, 380–386.

Reible, D.D., Popov, V., Valsaraj, K.T., Thibodeaux, L.J., Lin, F., Dikshit, M., Todaro, M.A., Fleeger, J.W., 1996. Contaminant fluxes from sediment due to tubificid oligochaetes bioturbation. *Wat. Res.* **30**, 704–714.

Reible, D., Mohanty, S., 2002. A levy flight-random walk model for bioturbation. *Environ. Toxicol. Chem.* **21**, 875–881.

Rice, D.L., 1986. Early diagenesis in bioadvective sediments: relationships between the diagenesis of beryllium-7, sediment reworking rates, and the abundance of conveyor-belt deposit-feeders. *J. Mar. Res.* **44**, 149–184.

Robbins, J.A., Kresoski, J.R., Mozley, S.C., 1977. Radioactivity in sediments of the Greats Lakes: post depositional redistribution by deposit-feeding organisms. *Earth Planet. Sci. Lett.* **36**, 325–333.

Robbins, J.A., 1986. A model for particle-selective transport of tracers in sediments with conveyor belt deposit feeders. *J. Geophys. Res.* **91**, 8542–8558.

Soetaert, K., Herman, P.M.J., Middleburg, J.J., Heip, C., DeStigter, H.S., Van Weering, T.C.E., Epping, E., Helder, W., 1996. Modeling ^{210}Pb-derived mixing activity in ocean margin sediments: diffusive versus nonlocal mixing. *J. Mar. Res.* **54**, 1207–1227.

Soster, F.M., Harvey, D.T., Troksa, M.R., Grooms, T., 1992. The effect of tubificid oligochaetes on the uptake of zinc by Lake Erie sediment. *Hydrobiologia* **248**, 249–348.

Stief, P., De Beer, D., 2002. Bioturbation effects of *Chironomus riparius* on the benthic *N*-cycle as measured using microsensors and microbiological assays. *Aquat. Micr. Ecol.* **27**, 175–185.

Timmermann, K., Banta, G.T., Larsen, J., Andersen, O., 2003. Modelling particle and solute transport in sediments inhabited by *Arenicola marina*. Effects of pyrene on transport processes. *Vie Milieu* **53**, 187–200.

Vale, C., Sundby, B., 1998. The interactions between living organisms and metals in intertidal and subtidal sediments. In: Langston, W.J., Bebianno, M.J. (Eds.), *Metal Metabolism in Aquatic Environments*. Chapman and Hall, London, UK, pp. 19–29.

Wallace, W.G., Lopez, G.R., Levinton, J.S., 1998. Cadmium resistance in an oligochaete and its effect on cadmium trophic transfer to an omnivorous shrimp. *Mar. Ecol. Prog. Ser.* **172**, 225–237.

Wang, X., Matisoff, G., 1997. Solute transport in sediments by a large freshwater oligochaete, *Branchiura sowerbyi. Environ. Sci. Technol.* **31**, 1926–1933.

Warren, L.A., Haack, E.A., 2001. Biogeochemical controls on metal behaviour in freshwater environments. *Earth-Sci. Rev.* **54**, 261–320.

Wood, L.W., 1975. Role of oligochaetes in the circulation of water and solutes across the mud water interface. *Verh. Int. Verein. Theor. Angew. Limnol.* **19**, 1530–1533.

Wijsman, J.W.M., Herman, P.M.J., Middelburg, J.J., Soetaert, K., 2002. A model for early diagenetic processes in sediments of the continental shelf of the Black Sea. *Estuar. Coast. Shelf S.* **54**, 403–421.